

Top influencers can be identified universally by combining classical centralities

Doina Bucur^{1,*}

¹University of Twente, Department of Computer Science, Drienerlolaan 5, 7522 NB Enschede, The Netherlands
*d.bucur@utwente.nl

ABSTRACT

Information flow, opinion, and epidemics spread over structured networks. When using individual node centrality indicators to predict which nodes will be among the top influencers or spreaders in a large network, no single centrality has consistently good predictive power across a set of 60 finite, diverse, static real-world topologies from six categories of social networks. We show that multi-centrality statistical classifiers, trained on a sample of the nodes from each network, are instead consistently predictive across diverse network cases. Certain pairs of centralities cooperate particularly well in statistically drawing the class boundary between the top spreaders and the rest: local centralities measuring the size of a node's neighbourhood combine well with global centralities such as the eigenvector centrality, closeness, or the core number. As a result, training classifiers with seven classical centralities leads to a nearly maximum average precision function (0.995).

Introduction

Social influence, news, as well as infectious disease diffuse in society, following links drawn between participants by frequent contact, mutual interests, collaboration, communication, or transportation. The *influence* of a single node in such a network is one way of capture the node's importance in terms of the dynamic diffusion process. It measures the extent to which the node, acting as the seed of a multi-hop diffusion process, will activate the rest of the network—this is the cascade size in the domain of online social networks, and the attack rate or outbreak size in epidemiology. Even when the network links are known and the process of diffusion can be measured or simulated, finding which topological characteristic allows a node to be influential remains a difficult task, because of the diversity of social-network topologies. We show a robust statistical method of *predicting top influencers*, or superspreaders, in real-world network topologies, combining a number of classic node centrality indicators in a single, interpretable model.

Most prior studies predict top influencers by a *ranking method*¹: the nodes in a network are ranked according to a single centrality, with the top assumed to be the best influencers. Then, the centralities themselves are compared and ranked by their performance as individual predictors of influence, with inconsistent results. For example, the degree centrality was found a weak predictor in early studies, over both simulated and measured diffusion^{2,3}. Over both the susceptible–infectious–recovered (SIR)⁴ diffusion model and measured diffusion, the top $f\%$ spreaders in a small number of networks were better predicted by their core numbers than by degree or betweenness centrality, regardless of the infection probability simulated^{5,6} (except at low f , where the degree was marginally more predictive). However, the good predictive power of the core number was later shown to not generalise, for SIR influence at or above the epidemic threshold at which diffusion reaches a sizeable fraction of the network. In road networks, the core number correlated little with the spreading ability of a node, while in social networks the degree and core number were either equally predictive⁷, or variably predictive: the core number was in some test cases the most predictive single centrality, other times the degree was better, and yet other times the best predictor varied with f ⁸. Over a test suite of ten networks, the eigenvector centrality was (on average across the networks tried) better than the core number⁹. In other developments, new or improved topological centrality indicators are defined and compared with classical ones^{7,10–20}. No single centrality is consistent in performance across realistic case studies¹.

We go in a different direction and show that classical centralities can be sufficient as predictors of influence, when teamed up as input variables to a *single, multi-variate statistical classifier*. Classifiers using two or more centralities are trained on sample nodes from each network, with node data including their centrality values and a binary target variable which shows whether or not the node is in the top $f\%$ of spreaders. Some centralities play well together, and draw a more accurate, two-dimensional decision boundary between the two classes of nodes, which outperforms the decision boundary drawn by any single-centrality ranker. When combining the seven classical centralities in this study, the average precision function and recognition rate across our test suite of 60 social networks and 20 values for f are 0.995 and 0.921.

Ideas around combining centrality indicators into a predictor of influence started in 2011. A metric equal to the betweenness

centrality of a node, divided by a power r of its degree (the unbiased betweenness²¹) was used to recognise the seed of a diffusion process; it was not successful on a real-world topology. Other methods^{22–24} are not applied beyond relatively small networks. More general, but not interpretable approaches^{25,26} aggregate the individual rankings of two or more centralities (or the centrality values), with coefficients based on the correlations between the rankings, or the information entropy of a centrality. This aggregation gave recognition rates above 0.7 in 16 networks with the susceptible–infectious (SI) diffusion model—with significant improvement (9–18%) over the best single ranking in five of these networks, and a lower 1–5% in the rest²⁵. No explanation was found for the performance of any additional centrality. Two recent studies showed that the spread size from single seed nodes can be predicted by nonlinear regressors using multiple centralities as features^{27,28}. Across the entire space of very small nonisomorphic networks (up to 10 nodes), one normalized spectral centrality (PageRank or Katz centrality) combined well with degree²⁷, and a clear regression map shows what centrality values predictably give superspreaders. While these studies first determined that there is added predictive value to centrality combinations, we improve their results by studying a large set of real-world test networks of sizes between 1000 and 70,000 nodes, and explaining which combinations make good predictors and why.

Results

We run an empirical study over 60 real-world examples of static network topologies (listed in Table 1 in Methods). The networks are directed, unweighted, and fall into six categories: human social networks (separately, online or offline), human networks formed by professional coauthorship or online communication, computer networks, and physical infrastructure. The influence of a node is the SIR spread size when the node is the seed of diffusion, estimated via Monte Carlo simulation (see Methods). Analyses are shown in this section for the SIR influence at the epidemic threshold λ_c for every network; they hold also above the epidemic threshold, at $1.5 \cdot \lambda_c$ (with numerical results for these shown in the Supplementary Information). We study seven classical centrality indicators and their combinations: the *degree*, *neighbourhood* (the sum of the degrees of direct neighbours), *two-hop neighbourhood* (the sum of the degrees of neighbours exactly two hops away), *core number* as resulted from k-shell decomposition, *PageRank*, *eigenvector* centrality, and *closeness* centrality.

The predictive power of single centralities is inconsistent across networks

We first show that the ability of any one centrality indicator to predict the top spreaders across a large number of network cases is too variable to be of universal practical use. Take a network of N nodes, f a fraction, and the task of selecting the best fN spreaders in the network. The standard ranking method has each centrality rank the nodes in this network; the top fN nodes by this ranking are put forward as best spreaders^{5–9} (see Methods). The predictive power of the degree centrality is shown in Fig. 1, across all networks, at the epidemic threshold. This is measured via the *recognition rate* (also called recall) $r(f)$: the fraction of correctly identified top spreaders (Eq. 1 in Methods); the 95% confidence interval around $r(f)$ is shown as a shaded area. In Fig. 1, for each of the three categories of networks with lowest recognition rates at $f = 20\%$, the worst-case network is named. The degree-influence scatterplots, also in Fig. 1, show the reason: a correlation between degree and influence does exist even in these worst cases, but with too wide a variance of influence per degree for accurate ranking.

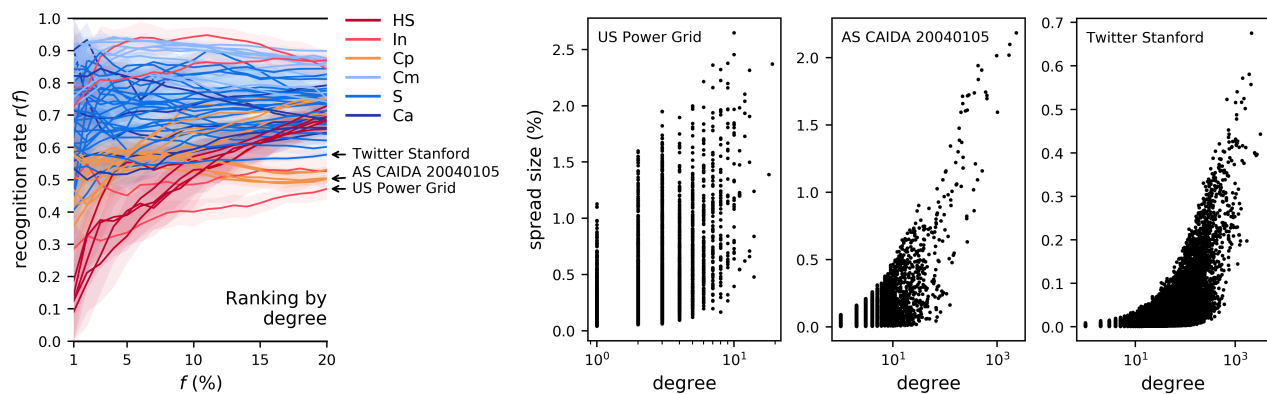


Figure 1. (left) The recognition rate by **degree**, across f , for all networks, at the SIR epidemic threshold. Each data line corresponds to a network, with the 95% confidence interval shown as a shaded, partly transparent area. The network categories are *Ca* (Coauthorship, 6 networks), *Cm* (Communication between people, 11 networks), *Cp* (Computer, 11 networks), *HS* (offline Human Social, 5 networks), *In* (Infrastructure, 4 networks), *S* (online Social, 23 networks). (right) Degree-influence scatterplots for three of the worst-case networks.

Compared to the degree, the performance of the core number as a ranker is much less consistent across networks (Fig. 2). The same cause holds for the three worst-case networks marked in the figure: all have few k-shells (between 1 and 5), so the core number by itself is not a discriminative variable for a ranking task. In the very worst case (as in the case of Gnutella25), the network has a single k-shell, so predicting the top spreaders by ranking the nodes in the network is the same as doing a random draw. In Fig. 2, three more networks are marked, for which ranking by core number gives good recognition rates at $f = 20\%$, but poor rates when $f < 5\%$. The scatterplots between core number and influence show the cause. The nodes with the highest core number in the Twitter Stanford network are poor spreaders; a topological reason for this was found in a prior study focused on the core number⁸: the most effective core in the network depends not only on its core number, but also on its connectivity to other cores. Even in other topologies, in which high core numbers do correlate with wide spreading (as is the case for Twitch ES and US Airports), the highest core contains many nodes of very variable influence, so the core number alone is not a sufficiently discriminative variable.

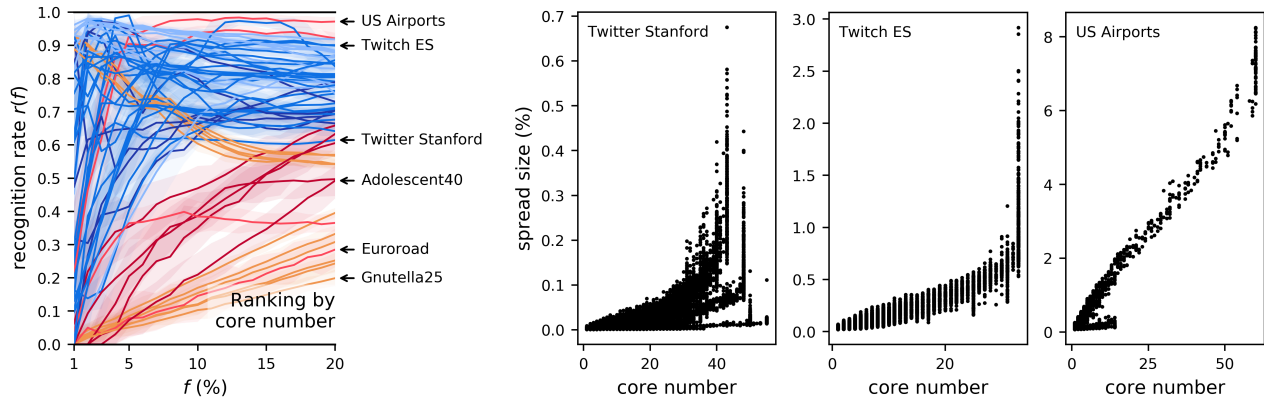


Figure 2. As Fig. 1, but with the **core number** as the ranker.

Neither the degree centrality nor the core number are universally better than the other across the network space. If the core number can be a more accurate ranker in some cases (Fig. 2 shows values of $r(f)$ closer to 1 for the core number, as was also found in prior studies on selected topologies^{5,6}), it is also a poor predictor in absolute terms when $f < 5\%$ for many networks, and also across all f values when the network doesn't have a strong core structure. For online human networks (categories Ca , Cm , and S in this study), and with $f > 5\%$, Figs. 1–2 show the two centralities to be comparable, with the core number marginally better; in general, as recognised before^{7–9}, the predictive power of the core number is not consistently better than the degree centrality for SIR influence.

Another popular ranker, the eigenvector centrality was previously found (on average across a set of networks) more predictive than the core number⁹. By the summary in Fig. 3, this is the case for low values of f , but there is still a wide variance between networks. In some cases (such as Gnutella24 and Euroroad, marked in the figure), the distribution of centrality values is such that ranking is not better than a random draw; in others, such as Adolescent40, there is little correlation between the centrality and influence, so the ranking remains poor. In the best of cases (for two of them scatterplots are shown in the figure), this correlation is strong, which explains why the eigenvector centrality can be a very good predictor across the range of f .

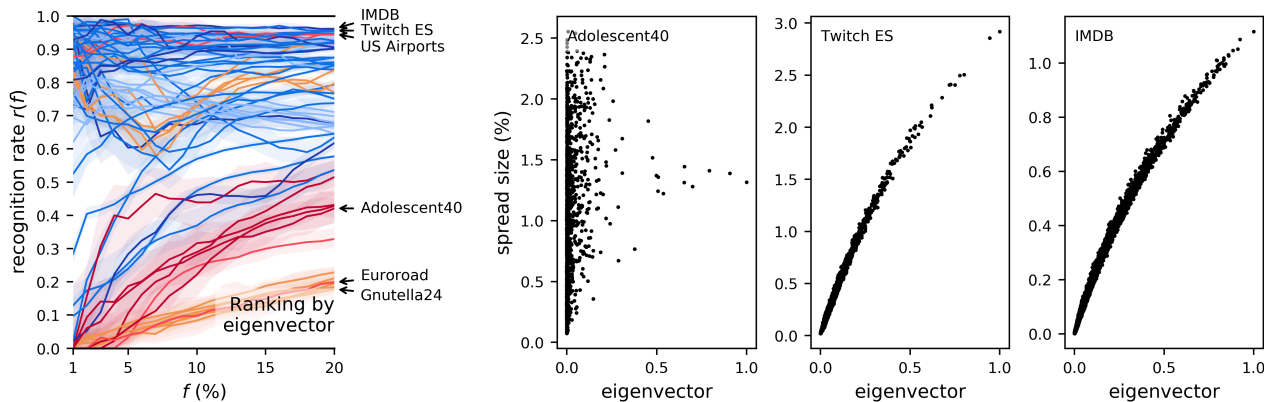


Figure 3. As Fig. 1, but with the **eigenvector centrality** as the ranker.

A second performance metric is also of interest: the *precision function* $p(f)$ (Eq. 1 in Methods), which compares the SIR influence of the predicted nodes with the SIR influence of the correct top spreaders. A $p(f)$ value close to 1 for a prediction task means that, regardless whether or not the exact top spreaders were identified, the influence of the nodes which were identified is close to that of the set of top spreaders—so $p(f)$ does not penalise node substitutions, if the substitutes are similar in terms of influence. For ranking by single centralities, the results for both the recognition rate and the precision function are shown in Fig. 4. Each data point marks the performance of a ranking task, over a given network, for a value of f in $1, 2, \dots, 20\%$. (To make the data points visible despite many partial overlaps, each data point is a horizontal line; this line does not denote the uncertainty of the data, but is of fixed size.) The centroid of each data cloud summarises the performance of that centrality over this set of networks. Overall, the neighbourhood centrality makes for the best single ranker, with an average recognition rate of 0.804 and an average precision function of 0.962. The two-hop neighbourhood (not shown in the figure) is only slightly worse (on average 0.781 and 0.942, respectively). PageRank is the least accurate, with an average recognition rate of 0.487, and an average precision function of 0.727. This latter result is not entirely surprising: although widely used for ranking nodes in network structures²⁹, PageRank was found before to not be a competitive predictor for measured diffusion in various networks^{6,9}.

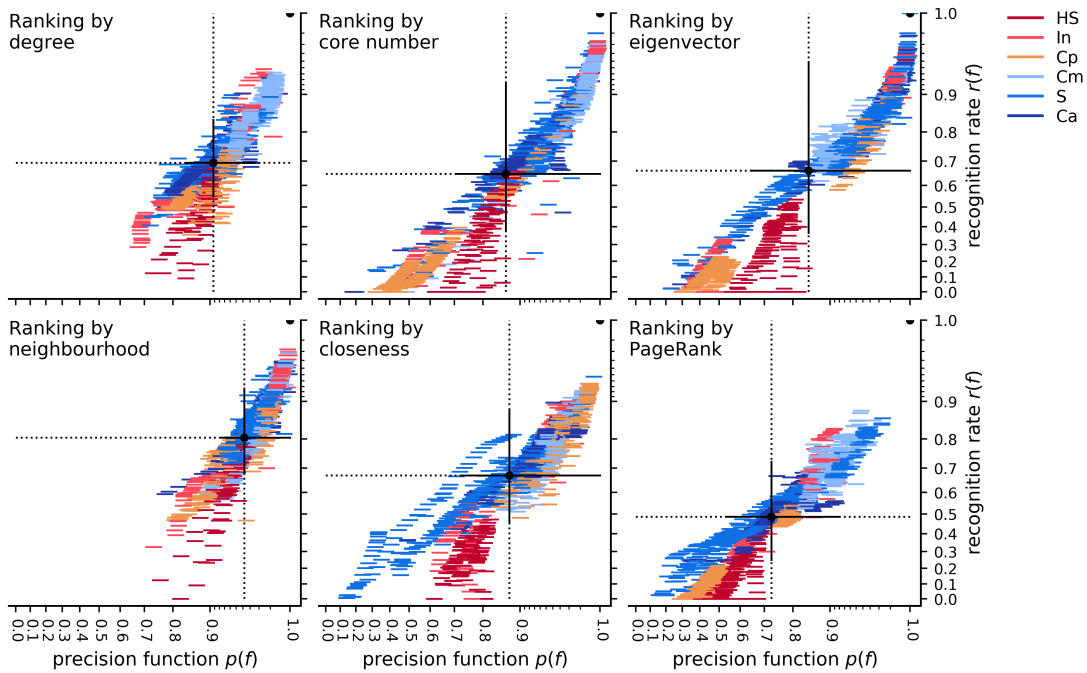


Figure 4. The success of **single-centrality ranking** at predicting spreaders, across all networks and values of f , at the SIR epidemic threshold. The scales are quadratic. Each data point (a horizontal line of fixed size) denotes a prediction task, and the colour shows the category of the network (listed in Table 1 in Methods). The centroid of the point cluster and the standard deviation on both axes are marked with a solid dot and lines. The point of perfect scores (1,1) is also marked with a half circle. The neighbourhood centrality is the best overall single ranker, with an average precision function of 0.962 and an average recognition rate of 0.804.

Next, we show that certain pairs of centrality indicators have, together, sufficient topological information about network nodes to improve the accuracy of the prediction tasks.

Pairs of centralities combine into better predictors

A statistical classifier is now trained with multi-variate data from part of the nodes in each network. The result is one trained classifier per network and fraction f . For training, a centrality is one input feature. The target variable (or class) is binary, and it shows whether or not a node is in the top fraction f in the network by spread size. The two performance metrics for the classifiers are the same as for ranking tasks, with the difference that the recall $r(f)$ is now improved as the F1 score, which is the harmonic mean between the precision of classification and the recall (for motivation, see Methods, Eq. 2). The statistical models trained are support-vector machine (SVM) with second-degree polynomials as kernels (see Methods), which always give simple, interpretable *decision boundaries* between classes. We also verified that the conclusions hold for other, higher-variance statistical models based on decision trees (with numerical results for these shown in the Supplementary Information).

We start with training SVM classifiers with two centralities, and show that, for certain network examples, certain pairs of centralities build on each other's strengths and obtain predictive models that are significantly better than either centrality alone. We show six such network examples in Fig. 5. For each network, the left panel maps the distribution of the spread size at the epidemic threshold for all the nodes in the network, against a chosen pair of centralities. The right panel notes a value for f , and colours the nodes according to their true class: the red nodes are the top f by spread size. Also in the right panel, two dotted lines show the decision boundaries made by the corresponding single-centrality rankers. If $f = 1\%$, these boundaries are the 99th percentiles for either centrality; a ranker will predict as top spreaders all nodes above this boundary. These ranking boundaries are improved upon by the classifier, whose decision boundary is shown as the transition between background colours, with a blue (darker) background showing the centrality space where the top spreaders are predicted to be. (Note that only part of this centrality space may be occupied by nodes; in other words, not every combination of centrality values may be physically possible.) The optimal decision boundary would leave no nodes misclassified and would lead to values of 1 for both the precision function and the recall or F1 score.

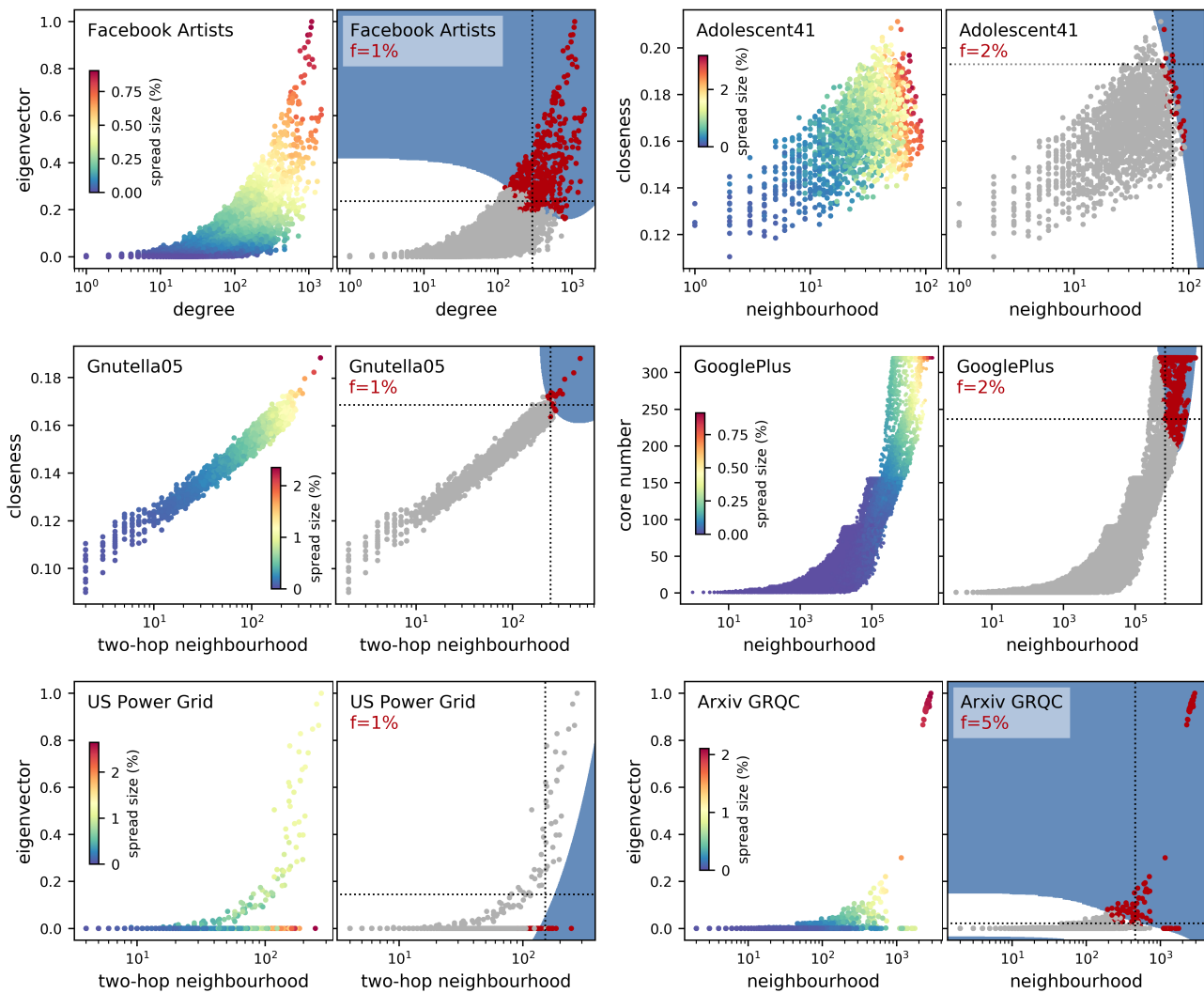


Figure 5. Six network examples for which **two-centrality classifiers** improve the predictions of single-centrality rankers. In every left panel, a scatterplot of node centralities versus spread size. In every right panel, the top spreaders are coloured in red (or darker), the decision boundaries for rankers using either centrality are dotted lines, and the background colour shows the decision boundaries for the classifiers: a blue (or darker) background denotes the area predicted for top spreaders.

In the examples from Fig. 5, each classifier's decision boundary improves upon the decision boundary of any ranker such that $r(f)$ is raised by (in increasing order over the examples in the figure) between 0.090 and 0.213. In the example of the Facebook Artists network, ranking the nodes by only degree or only the eigenvector centrality places many nodes close to the

decision boundary in the wrong class; unlike a single-centrality ranker, the degree-eigenvector classifier (F1 score of 0.925) draws a decision boundary that is much closer to optimal. The same is the case for the remaining five examples, each with a different pair of centralities, and with all centralities except PageRank represented in these pairs. (PageRank is present in such successful pairs of centralities, but less frequently.) In particular, the example of the GooglePlus network when $f = 2\%$ (F1 score of 0.970) shows how the problems that the core number has with discriminating top spreaders (Fig. 2) are now resolved with help from the neighbourhood centrality: while the core number performs a rough selection of the nodes, with higher cores more likely to have larger influence, the neighbourhood centrality refines this selection.

Among our 60 test cases, we also found other examples of networks, combined with certain values for f , for which the single-centrality rankers could not be improved by any classifier. When $f = 1\%$, none of the five Adolescent networks is resolved any better by using two centralities. This can change for different values of f . At $f = 2\%$, for the Adolescent41 network (shown in Fig. 5), the combination of neighbourhood and closeness improves recall by 0.129, to reach an F1 score of 0.635.

From all pairs of centralities, the combination of two-hop neighbourhood and core number has the best average F1 score (0.865) across all the network cases in this study, and across the range of f . On the other hand, the combination of two-hop neighbourhood and eigenvector has the best average precision function (0.992). Figure 6 is a summary for the averages of both performance scores across all single centralities (on the diagonal) and pairs of centralities (the rest of the matrix). All possible pairs of centralities are studied, except for the redundant combinations between degree and neighbourhood, and between the two types of neighbourhood centralities. The six pairs which improve significantly on the most predictive ranker are all composed of one of the neighbourhood centralities, and one of: core number, eigenvector centrality, closeness, or PageRank. These six pairs improve on both recall and precision function.

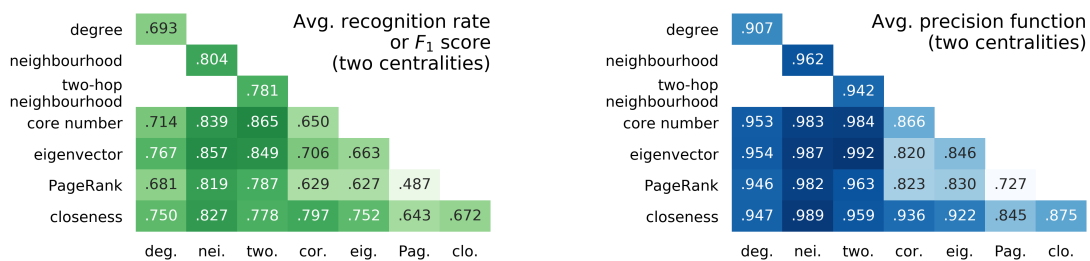


Figure 6. The success of **single and pairs of centralities** at predicting spreaders: for each pair of centralities, the average performance score across all networks and values of f . The diagonal is the result of ranking by a single centrality and it is scored by the recognition rate and the precision function. The rest of the matrix is the result of classification by two centralities and is scored by the F1 score and the precision function.

Multi-centrality predictors and summary of results

While the previous subsection demonstrated that centrality indicators can play on each others' strengths and improve the prediction of top spreaders by the ISR diffusion model at the critical threshold, we now show that classifiers using all seven centralities as features give near-perfect prediction on most network examples, with the exception of offline human social networks (the HS network category) at low fractions f .

We train a seven-centrality SVM classifier for each prediction task, and summarise the results in Fig. 7. The centroid of all prediction scores (Fig. 7, left) is an average recognition rate of 0.921, and an average precision function of 0.995. While the precision function was almost as high (0.992) when training the classifier using only the eigenvector centrality and the two-hop neighbourhood as features (Fig. 6), the average recognition rate is now further improved by adding more features to the statistical model. Not all six network categories are equal: a breakdown of the scores by network category and by the value of the fraction f (Fig. 7, right) shows that recognising the top 1% of spreaders in the Adolescent networks (the HS network category) remains difficult. All other prediction tasks are resolved well, particularly when performance is measured by the precision function, which ranges between 0.969 and 1.

These conclusion hold also above the epidemic threshold, at $1.5 \cdot \lambda_c$; numerical results showing very similar prediction scores are in Supplementary Figure S1. They are also not an artefact of the type of statistical model used in the classifier (an SVM with a second-degree polynomial kernel, which we selected based on it learning clear, interpretable decision boundaries). When training nonlinear Random Forest classifiers, which are high-variance so—in general—are able to obtain better performance than the polynomial SVM, a similar conclusion emerges (Supplementary Figure S2).

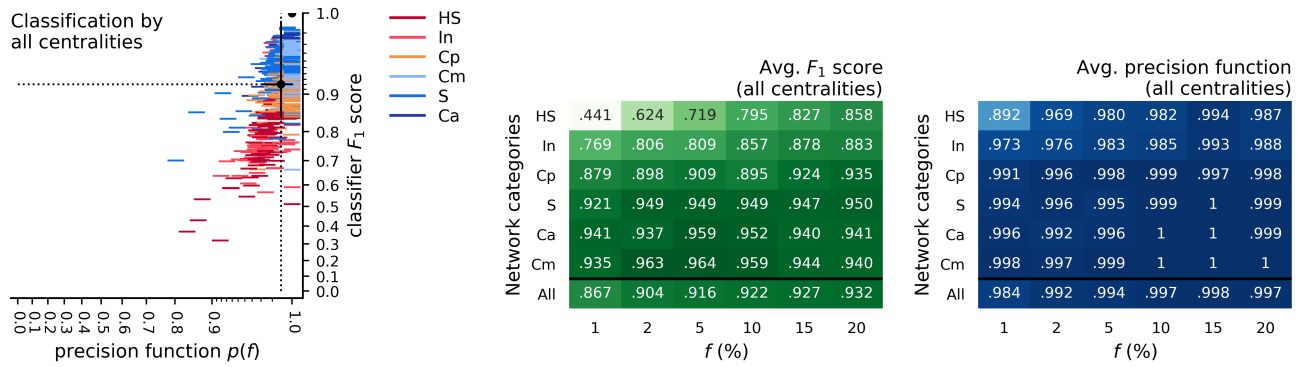


Figure 7. The success of **classifiers using all centralities** at predicting spreaders, across all networks and values of f , at the SIR epidemic threshold. (left) Each data point denotes a prediction task, and the colour shows the category of the network (listed in Table 1). The centroid of the point cluster and the standard deviation on both axes are marked (counterpart to Fig. 4). (right) The average performance scores across all networks in one of six network categories, and across all values of f (counterpart to Fig. 6).

Discussion

In this study, we showed that classical node centrality indicators, often assumed to be good proxies for various measures of dynamical node importance, are not universally accurate at predicting which nodes will be among the top spreaders when seeding an SIR diffusion process. On the other hand, we showed a solution for this prediction task: when combined into an interpretable, machine-learned statistical classifier, two or more of the same classical centrality indicators can contain sufficient statistical information about the nodes to make an accurate predictor of SIR influence.

The decision boundaries between the two classes, as learnt by classifiers, demonstrate where the advantage of multi-variate prediction comes from: certain centrality indicators are particularly good complements to others. For the degree centrality, the best complement (on average across the 60 networks in this study) is the eigenvector centrality. For the neighbourhood centrality (which is also the best overall single ranker, despite it being an easy to estimate, local centrality), three other centralities make good complements: the eigenvector centrality, closeness, and core number (with PageRank also close). For those network cases where multi-variate prediction has an advantage, the joint distribution of the centralities and the SIR influence is such that one centrality (or, a one-dimensional decision boundary) is insufficient to classify the nodes accurately, but a multi-dimensional decision boundary is able to refine the decision in the most important region of centrality values. Notably, there are multiple answers to the question: what is a good pair of centralities? Either one of the two neighbourhood measures can be used together with either an eigenvector-based measure, the core number, or the closeness centrality.

This method is practical. For a given network, a statistical classifier is trained on a sample of the nodes in the network, and will predict which of the other nodes fall into the category of superspreaders. Ground truth for the target variable (the influence of a node) to be used as training data can be obtained either (a) empirically, by measuring the outcome of similar diffusion processes from the history of the same social network, or (b) via the simulation of the dynamic process on randomly sampled nodes in the network (as in this study). The size of the training data necessary to obtain good predictions depends on the network, and on the distributions of centrality and influence values. In Supplementary Figure S3, we give learning curves for three of the largest networks in this study (they show that some networks only require a training data size of 1% of the network size, while others need around 10%). The set of centralities to use as features can be tailored to the computational budget available. The type of statistical model can be tailored with the network size: heuristic training algorithms, such as those training Random Forest classifiers, scale better with large networks.

There are follow-ups to explore as continuations of this study, still at the intersection between real-world network dynamics and machine learning: the prediction of other measures of node influence (such as the measured diffusion of information in large online social networks⁶) and of node importance (such as the ability of a node to block the diffusion of information), and the study of other types of networks (such as different network categories, networks with node attributes, and networks with dynamic structure).

Methods

Networks, centrality indicators, and the estimation of node influence

Most of the networks used as case studies (see Table 1 for the overview) model entire communities at a specific point in time. This is the case for the high-school friendships in the Adolescent networks, the daily Gnutella peer-to-peer file sharing networks, the five sets of institutional email exchanges, or the networks of mutual likes between verified Facebook pages. A minority of the networks (such as the Facebook Stanford friendships, collected from survey participants) are instead bounded samples from a larger community. All are (transformed into) directed, strongly connected, and unweighted networks; when the original version in the repository had timestamp, attribute, or weight annotations, these were removed. The direction of the edges is reversed when needed, to model information flow—so the degree centrality of interest is the out-degree. To be able to study the closeness centrality³⁰ which computes the lengths of shortest paths, only the largest strongly connected component (SCC) was kept. These networks were selected from public repositories such that (a) they fit into these six categories, and (b) have the size of their SCC above 1,000 nodes. The upper bound on network size is simply imposed by finite computing resources.

Cat.	Rep.	Network	Size	λ_c	Cat.	Rep.	Network	Size	λ_c
HS	K	Adolescent36	1,671	0.29	S	S	Facebook Public Figures	11,565	0.020
HS	K	Adolescent40	1,679	0.23	S	S	Facebook Stanford	4,039	0.011
HS	K	Adolescent41	1,640	0.26	S	S	Facebook TV Shows	3,892	0.049
HS	K	Adolescent49	1,149	0.25	S	S	GitHub	37,700	0.0105
HS	K	Adolescent50	2,155	0.25	Cp	S	Gnutella04	4,317	0.29
S	K	Advogato	3,140	0.041	Cp	S	Gnutella05	3,234	0.32
Ca	S	Arxiv Astro	17,903	0.0155	Cp	S	Gnutella24	6,352	0.39
Ca	S	Arxiv CondMat	21,363	0.045	Cp	S	Gnutella25	5,153	0.42
Ca	S	Arxiv GRQC	4,158	0.080	Cp	S	Gnutella30	8,490	0.35
Ca	S	Arxiv HEPPh	11,204	0.008	Cp	S	Gnutella31	14,149	0.38
Ca	S	Arxiv HEPTh	8,638	0.0925	S	S	GooglePlus	69,501	0.0019
Cp	S	AS CAIDA 20040105	16,301	0.033	S	K	Hamsterster	2,000	0.029
Cp	S	AS CAIDA 20041206	18,501	0.028	Ca	M	IMDB	47,719	0.003
Cp	S	AS CAIDA 20051205	20,889	0.028	In	K	OpenFlights	3,354	0.024
Cp	S	AS CAIDA 20061225	23,918	0.027	S	K	PGP	10,680	0.065
Cp	S	AS CAIDA 20071112	26,389	0.030	S	S	Twitch DE	9,498	0.0085
S	S	Brightkite	56,739	0.0185	S	S	Twitch EN	7,126	0.033
Cm	S	Email Enron	33,696	0.012	S	S	Twitch ES	4,648	0.014
Cm	S	Email EU	34,203	0.022	S	S	Twitch FR	6,549	0.0098
Cm	K	Email Linux	18,531	0.0075	S	S	Twitch RU	4,385	0.0185
Cm	M	Email UCL	12,625	0.035	S	S	Twitch PT	1,912	0.013
Cm	K	Email URV	1,133	0.070	S	S	Twitter Stanford	68,413	0.0115
S	S	Epinions	32,223	0.0135	In	K	US Airports	1,402	0.020
In	K	Euroroad	1,039	1.3	In	K	US Power Grid	4,941	0.87
S	S	Facebook Artists	50,515	0.007	Cm	K	WikiTalk AR	8,797	0.018
S	S	Facebook Athletes	13,866	0.030	Cm	K	WikiTalk IT	36,356	0.008
S	S	Facebook Companies	14,113	0.057	Cm	K	WikiTalk NL	18,598	0.012
S	S	Facebook Government	7,057	0.014	Cm	K	WikiTalk PT	21,747	0.009
S	M	Facebook New Orleans	63,392	0.0098	Cm	K	WikiTalk RU	22,664	0.011
S	S	Facebook Politicians	5,908	0.031	Cm	K	WikiTalk ZH	10,831	0.013

Table 1. The 60 case studies. We use the largest strongly connected component, whose size (node count) is reported here. **Rep.** denotes the source repository: *K* (KONECT^{31,32}), *M* (H. Makse³³), or *S* (SNAP³⁴). **Cat.** is the KONECT category most suited to the case study: *Ca* (Coauthorship), *Cm* (Communication between people), *Cp* (Computer), *HS* (Human Social, offline), *In* (Infrastructure), *S* (Social, online). λ_c denotes the epidemic threshold, estimated numerically.

The following centrality indicators were computed for every node in every network: its *degree*, *neighbourhood* (i.e., the sum of the degrees of the nearest neighbours, previously denoted k_{sum} and found to be a competitive predictor in a previous study⁶), *two-hop neighbourhood* (as before⁶ for nearest neighbours exactly two hops away and previously denoted k_{2sum}), *PageRank*³⁰ with a 0.85 damping factor, *eigenvector centrality*³⁰, *closeness centrality*³⁰, and *core number*⁵. An additional set of indicators that we tried, the *link strength* of a node towards upper, equal, or lower shells⁸, denoted r^u , r^e , or r^l , did not provide notable results.

The ultimate influence of a node in a network is estimated numerically, as the average among 10^4 runs of the susceptible–infectious–recovered (SIR)⁴ diffusion model for infectious diseases. In SIR, an infectious node infects a susceptible neighbour at a rate β (meaning the number of infection events per time unit, so can be higher than 1). An infectious node recovers at a rate μ . The effective transmission rate is $\lambda = \beta/\mu$. Here, we take $\mu = 1$ and study the normalized rate λ .

As λ increases in SIR simulations, the size of the outbreaks increase from an infinitesimal fraction to a finite fraction of the network size. The regime of interest is neither very low λ values (in which case, the diffusion remains localised to the

neighbourhood of the seed node) nor very high (in which case, all nodes should reach a large fraction of the network). Since our test cases are both finite in size, and diverse (a scenario studied previously³⁵), we estimate the *epidemic threshold* λ_c numerically by identifying it with the variability measure³⁵ $\Delta = \frac{\sqrt{\langle \rho^2 \rangle - \langle \rho \rangle^2}}{\langle \rho \rangle}$. Here, ρ denotes the random variable of outbreak size from different seed nodes, and $\langle \cdot \rangle$ denotes the mean. Given a value for λ , Δ is estimated by setting seed nodes from a random sample of 10^4 of the nodes in a network (or the entire network size, if this is smaller). After estimating Δ for a range of λ values at regularly spaced intervals, we take λ_c to be the position of the peak of Δ . The resulting values are noted in Table 1. The maximum spread size (influence) at λ_c in any network is between 0.7% and 6% of the network size (with two exceptions among the smallest infrastructure networks, where this reaches 8% and 11%).

Ranking by a single centrality

Method We first predict superspreaders using the single-centrality ranking method common in prior studies⁵⁻⁹, and also carry forward the performance metrics defined in these studies. This ranking method builds the assumption that higher centrality values for a node will also indicate higher node influence. Given a centrality C , first all the nodes have their values for C computed. The top fraction f of spreaders is then predicted to be the fraction f of nodes with the highest values for C . At ties between nodes (which occur for discrete-valued centralities such as degree and core number) a random subset of the tied nodes are selected. This random sampling is then repeated 10^2 times for a bootstrap technique (described below), which averages among the scores of these individual random choices.

Performance metrics In prior studies, this ranking is evaluated via two metrics. Denote by I_f the set of the top fraction f of nodes as ranked by their SIR influence, and by C_f the set of top fraction f of nodes as ranked by their centrality values; the sizes of these sets are equal for a given f , $|I_f| = |C_f|$. Also denote by ρ_i the spread size when setting node i as seed. The *recognition rate* $r(f)$ measures the extent to which the identities of the predicted superspreaders match the true identities⁶. A synonym for the recognition rate is *recall*. The *precision function* $p(f)$ is a weaker, but more practically useful performance measure comparing the spread of the predicted superspreaders to that of the true top spreaders:

$$r(f) = \frac{|I_f \cap C_f|}{|I_f|} \quad \text{and} \quad p(f) = \frac{\text{avg}_{i \in C_f} \rho_i}{\text{avg}_{i \in I_f} \rho_i} \quad (1)$$

Both metrics take values in the interval $[0, 1]$. An imprecision function $\varepsilon(f)$ was defined previously⁵, such that lower values of $\varepsilon(f)$ are better. Here, to present the two metrics in a unified fashion, we use instead $p(f) = 1 - \varepsilon(f)$, such that higher values are better for both $r(f)$ and $p(f)$. A confidence interval was originally provided for $r(f)$ by bootstrap⁶. Here, we apply a bootstrap technique when estimating both metrics. Given a network of N nodes, 10^2 times, we draw a random sample of the N nodes uniformly with replacement. Among these nodes, the ranking method is applied and a prediction is made and evaluated via either $r(f)$ or $p(f)$, as needed. The final value for each performance metric is the average, together with the 95% confidence interval among these samples.

Classification by a combination of centralities

Method A multi-centrality method learns a *discriminative statistical model* able to classify network nodes into superspreaders or not. For this, a dataset is formed for every network; a record describes a node via its centrality values (the predictors). When training the model to recognise the top fraction f of the nodes, the nodes are ranked by their true SIR spread size, and each node is assigned one of two target classes based on whether or not they are in the top fraction f . The model is trained and tuned on a training fraction $t = 0.5$ of the nodes (sampled randomly without replacement), and tested on the remaining nodes.

A binary statistical classifier learns a decision boundary between the classes. We use a *support-vector machine* (SVM)³⁶, which learns optimal separating hyperplanes in the multi-dimensional predictor space, including in cases where the classes overlap in this space. Here, the optimal decision boundary is that which leaves the largest margin in space between the classes, with still allowing some data points to fall on the wrong side of the boundary. SVMs have advantages: (a) they are optimal learners rather than heuristics, and (b) the kernel function K and the regularisation parameter C , which ultimately give the shape and variance of the boundary³⁷, are tunable hyperparameters.

We aim to obtain the simplest (and thus most interpretable) classifier with good performance. The results presented are for second-degree polynomials K (which gives a low-variance model, less prone to overfitting), C tuned in the range $[1, 100]$ with five-fold cross-validation, and a fixed tolerance for the stopping criterion³⁸ of $5e-4$. No class weights are added to balance the classes artificially. (We tested other, higher-variance statistical models: SVMs with third-degree polynomials for K , and models based on decision trees, either boosted or in ensembles³⁹; since they had similar performance to the SVM with a second-degree polynomial for kernel, we retain and present the results for the latter.) We show the decision boundaries learnt by two-centrality models via plotting them in the predictor space.

Performance metrics For a network of size N and the fraction f , a classifier produces a guess for the class of each network node in the test set. We port the same notation C_f to mean here the set of nodes classified as top spreaders. The number of superspreaders predicted in this way is decided by the classifier, and may not equal fN . We measure the overlap between the classifier prediction and the ground truth with metrics similar to Eq. 1. In binary classification, the measure $r(f)$ as defined in Eq. 1 is called *recall* or sensitivity. It is a useful metric, but insufficient to characterise the classifier: alongside making many correct choices (giving a high true positive rate, $|I_f \cap C_f|$), the classifier may also add many false positives. The *precision* metric helps to quantify the false positives, and a classical metric is the combination of recall and precision is their harmonic mean, the *F1 score*⁴⁰:

$$\text{recall}(f) = r(f) = \frac{|I_f \cap C_f|}{|I_f|} \quad \text{precision}(f) = \frac{|I_f \cap C_f|}{|C_f|} \quad \text{F1 score}(f) = \frac{2}{\text{recall}(f)^{-1} + \text{precision}(f)^{-1}} \quad (2)$$

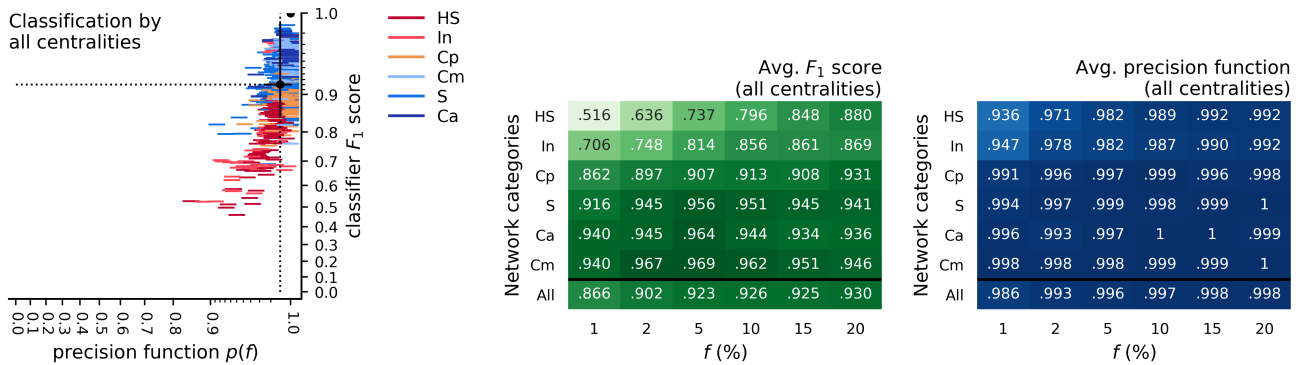
Note that *precision* is an established name in the area of Information Retrieval⁴⁰, while the *imprecision function* $\epsilon(f)$ which gave the *precision function* $p(f)$ was defined recently⁵ for analysing networks. Although the names are unfortunately too similar, their meaning is different and should not be confused.

The F1 score takes values in the interval $[0, 1]$. We apply to the classifier the second metric, the precision function $p(f)$, exactly as it is defined in Eq. 1. Its values can exceed 1.0, in cases when the classifier predicts fewer than fN superspreaders, and they are on average better than the true fN superspreaders; we cap higher values to 1.0. We estimate both F1 score and $p(f)$ by randomly drawing different training sets for the classifier (the same training fractions t of the nodes) 10^2 times, then training and testing the classifier on each draw. The final value for each performance metric is the average of the individual scores.

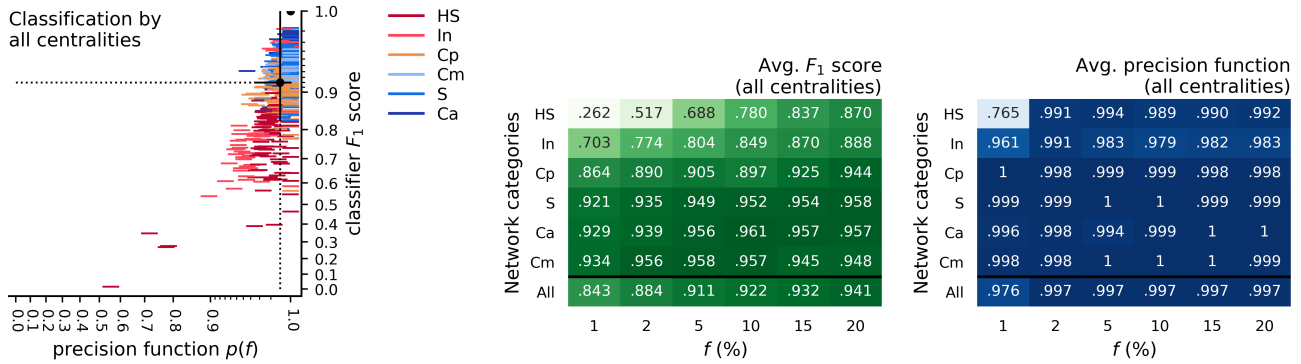
References

1. Mariani, M. S. & Lü, L. Network-based ranking in social systems: three challenges. *J. Physics: Complex.* **1**, 011001 (2020).
2. Watts, D. J. & Dodds, P. S. Influentials, networks, and public opinion formation. *J. consumer research* **34**, 441–458 (2007).
3. Cha, M., Haddadi, H., Benevenuto, F. & Gummadi, K. P. Measuring user influence in Twitter: The million follower fallacy. In *fourth international AAAI conference on weblogs and social media* (2010).
4. Anderson, R. M. & May, R. M. Population biology of infectious diseases: Part I. *Nature* **280**, 361–367 (1979).
5. Kitsak, M. *et al.* Identification of influential spreaders in complex networks. *Nat. physics* **6**, 888–893 (2010).
6. Pei, S., Muchnik, L., Andrade Jr, J. S., Zheng, Z. & Makse, H. A. Searching for superspreaders of information in real-world social media. *Sci. reports* **4**, 5547 (2014).
7. De Arruda, G. F. *et al.* Role of centrality for the identification of influential spreaders in complex networks. *Phys. Rev. E* **90**, 032812 (2014).
8. Liu, Y., Tang, M., Zhou, T. & Do, Y. Core-like groups result in invalidation of identifying super-spreader by k-shell decomposition. *Sci. reports* **5**, 9602 (2015).
9. Macdonald, B., Shakarian, P., Howard, N. & Moores, G. Spreaders in the network SIR model: An empirical study. *arXiv preprint arXiv:1208.4269* (2012).
10. Lü, L., Zhang, Y.-C., Yeung, C. H. & Zhou, T. Leaders in social networks, the Delicious case. *PloS one* **6** (2011).
11. Garas, A., Schweitzer, F. & Havlin, S. A k-shell decomposition method for weighted networks. *New J. Phys.* **14**, 083030 (2012).
12. Chen, D.-B., Gao, H., Lü, L. & Zhou, T. Identifying influential nodes in large-scale directed networks: the role of clustering. *PloS one* **8** (2013).
13. Zeng, A. & Zhang, C.-J. Ranking spreaders by decomposing complex networks. *Phys. Lett. A* **377**, 1031–1035 (2013).
14. Liu, J.-G., Ren, Z.-M. & Guo, Q. Ranking the spreading influence in complex networks. *Phys. A: Stat. Mech. its Appl.* **392**, 4154–4159 (2013).
15. Chen, D.-B., Xiao, R., Zeng, A. & Zhang, Y.-C. Path diversity improves the identification of influential spreaders. *EPL (Europhysics Lett.)* **104**, 68006 (2014).
16. Liu, Y., Tang, M., Zhou, T. & Do, Y. Improving the accuracy of the k-shell method by removing redundant links: From a perspective of spreading dynamics. *Sci. reports* **5**, 13172 (2015).

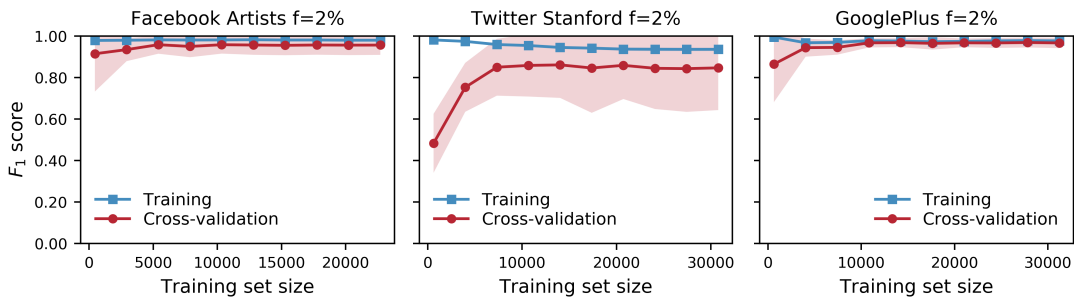
Supplementary Information



Supplementary Figure S1. The success of SVM classifiers using all centralities at predicting spreaders, across all networks and values of f , above the SIR epidemic threshold, at $1.5 \cdot \lambda_c$ for each network. (Counterpart to the summary results at the epidemic threshold λ_c from Figure 7).



Supplementary Figure S2. The success of Random Forest classifiers using all centralities at predicting spreaders, across all networks and values of f , at the SIR epidemic threshold λ_c for each network. (Counterpart to the summary results for SVM classifiers at the epidemic threshold λ_c from Figure 7).



Supplementary Figure S3. Learning curves for three large networks, showing the amount of training data (in terms of the number of nodes, on the x axis) versus the performance after training and cross-validation with all centralities (on the y axis). The training set size ranges between 1% and 50% of the network size, for each network. One can choose the size of the training data; a size is sufficient if the learning curve shows a high cross-validation score, close to the training score.